

21. Quintana-Murci, L., Semino, O., Bandelt, H.-J., Passarino, G., McElreavey, K. and Santachiara-Benerecetti, A. S., *Nature Genet.*, 1999, **23**, 437–441.
22. Torroni, A., Lott, M. T., Cabell, M. F., Chen, Y. S., Lavergne, L. and Wallace, D. C., *Am. J. Hum. Genet.*, 1994, **55**, 760–776.
23. Kivisild, T. *et al.*, *Curr. Biol.*, 1999, **9**, 1331–1334.
24. Chen, Y.-S., Olckers, A., Schurr, T. G., Kogelnik, A. M., Huoponen, K. and Wallace, D. C., *Am. J. Hum. Genet.*, 2000, **66**, 1362–1383.

ACKNOWLEDGEMENTS. D.E. is thankful to the Council of Scientific and Industrial Research for the award of Senior Research Fellowship. This study is supported by a grant from the Department of Biotechnology, Government of India. We also thank the members of the laboratory at the Anthropology and Human Genetics Unit of the Indian Statistical Institute, Kolkata for their help at various stages of this work.

Received 4 December 2001; accepted 27 June 2002

Aeromagnetic data to probe the Dharwar craton

S. P. Anand and Mita Rajaram*

Indian Institute of Geomagnetism, Colaba, Mumbai 400 005, India

Degree-sheet aeromagnetic maps of Dharwar craton were digitized closely along contours and re-gridded at 2.5 km interval to obtain an image map, after removal of International Geomagnetic Reference Field. The total field anomaly and generated analytical signal maps confirm the division of Dharwar craton into western and eastern blocks, and are consistent with the several strike trends of the causative sources. The Chitradurga schist belt appears to divide the Dharwar craton into the western and eastern blocks. From the present study we find that the density of the anomalies in the Eastern Dharwar is greater than that in the Western Dharwar. This may be explained by either or a combination of the following: higher grade of metamorphic rocks in the Eastern Dharwar or the Eastern block may be uplifted with respect to the Western block with the characteristics of the deeper crustal layer now exposed due to erosion or presence of thick sedimentary sequence in the Western with volcanic in the Eastern.

THE Dharwar craton, named by Pichamuthu¹, is one of the oldest Precambrian terrains of the world preserving within its limit the geological history of a very ancient (3400 to 2600 Ma) continental crust. The Dharwar craton is well known for its granite–greenstone association and it extends over an area of 350,000 km², covering the states of Karnataka and part of Andhra Pradesh. It is

delimited on the west by the present-day coastline and on the south and east by the dominantly Proterozoic high-grade. In the north it is bounded by the Bhima and Kaladgi basins and the Deccan volcanic province. Detailed geochemical and geophysical investigation of the granite–greenstone belts is important from the point of view of the reconstruction of the mineralization, tectonic history, grades of metamorphism, etc. of the Dharwar craton. Towards this end, the analysis of magnetic data can give a new perspective to probe the Dharwar craton.

Aeromagnetic degree-sheets up to 17°N were acquired from Geological Survey of India (GSI). These maps were re-digitized manually at 6' (10 km) interval and processed, mainly to study the long-wavelength features. Initial results were published by Harikumar *et al.*². In this paper the authors delineate the orthopyroxene isograd, demarcating the NW–SE trending Dharwar block to the north and the E–W trending Southern Granulate Terrain (SGT) block to the south of it. The source rock of magnetic anomalies is charnockites in the SGT and mainly intrusives and iron-ore bodies in the Dharwar craton. With the availability of machine digitization, it is possible to have these analogue degree-sheets in digital format. Such a format is used for analysing these maps critically to derive more useful information regarding structural trends, position of faults, distribution of shallow or deep crystalline basement, and occurrence of volcanic rocks within the sedimentary region, etc. The study of the spatial distribution of magnetic field facilitates the understanding of the regional as well as the global tectonic features. A new set of fine-grid aeromagnetic data, digitized closely along contours, is presented that helps to delineate the structural elements and distribution of magnetic sources in the Dharwar craton and to throw light on the magnetic properties of the oldest greenstone belt.

To be able to appreciate the block structures, we have chosen to restrict the area of study from just south of orthopyroxene isograd (line that divides the high-grade granulites to the south); thus data are taken from 12 to 17°N and 74 to 81°E. This includes the Dharwar craton, the Cuddapah basin and a part of the Eastern Ghats block.

Dharwar craton is divided into Eastern, Kolar-type and Western Dharwar-type blocks distinguished by differences in the volcano-sedimentary supracrustals, magmatism, grades of metamorphism and temporal evolution. Isotopic age studies using K–Ar, Rb–Sr and Pb–Pb methods placed the Western Dharwar craton (3000 Ma) to be older than the Eastern block³ (2500–2600 Ma). Some workers^{4,5} believe that the Closepet granite massif marks the boundary between Eastern and Western Dharwar, while others³ are of the opinion that the eastern boundary fault of the Chitradurga basin demarcates the two. Various views are put forth regarding the evolution of Dhar-

*For correspondence. (e-mail: mita@iig.iigm.res.in)

war craton⁶. The most characteristic structural feature of the Archean cover sequence of the Dharwar craton is the arcuate NNW–SSE trend with convexity towards the east. The major geological features in the Dharwar craton include the Archean–Early Proterozoic greenschist belts set in a matrix of Peninsular Gneiss–Migmatitic complex and the intrusive, younger potash-rich granites.

The Western Dharwar craton, a typical Archean low-grade terrain, is characterized by the mature sediment-dominated greenstone belt of the Dharwar type. Two main divisions, viz. the older igneous Bababudan group and the Chitradurga group composed of conglomerates, quartzites, limestones, greywackes and associated manganeseiferous and ferruginous cherts, are identified. These groups of sediments are deposited in three basins: the Shimoga, the Chitradurga and the Sandur basins. Banded iron-ore formations are exposed in the southern part of Shimoga basin in the Bababudan and Kudremukh belt in addition to Sandur and Goa basins. Magnetite, quartz and clay are the main mineral components of the iron-ore formations. The development of iron-formation points to stable conditions. In Figure 1, the iron-ore belts in the

Dharwar craton mapped under Project Vasundra³ are superposed on the geology map of the region.

The Eastern Dharwar block, comprising the Kolar-type schist belts, is typified by volcanic dominated greenstone belt (Keewatian type) characterized by low-pressure metamorphism. The prominent schist belts trending NNW–SSE are volcanogenic⁶ with thick pile of basalts and subordinate clastic and chemical sediment. These are known for their gold mineralization. They are mainly igneous in character with very subordinate sedimentary intercalations⁶. The major belts in the Kolar type include Kolar, Veligullu–Ramagiri, Hutti–Muski, Hungund–Kushtagi and Raichur–Deodurg⁶ (see Figure 1).

In the Eastern Ghats block (till the coastline), lithological assemblages vary from Archean to Recent. The basement constitutes mainly Proterozoic high-grade gneiss-granulites consisting of charnockites, khondalites and high-grade gneiss. Towards the coast, Recent alluvium is exposed. The study area also includes the western part of the Proterozoic sediment-covered Cuddapah basin and the volcano sedimentary-dominated Nellore-type schist belt forming the major thrust along the eastern

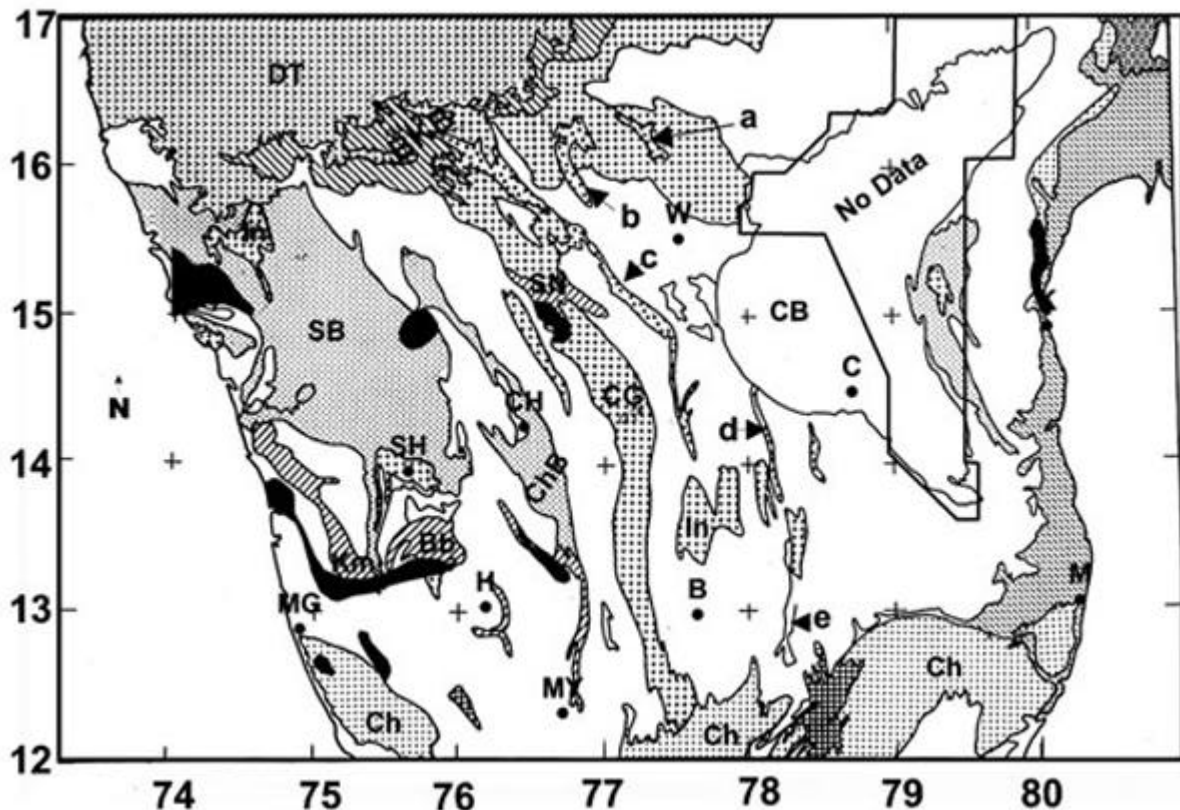


Figure 1. Geology and tectonic map of the study area redrawn from *Seismotectonic Atlas*⁷ and Project Vasundra³. B, Bangalore; C, Cuddapah; CH, Chitradurga; H, Hassan; K, Kavali; M, Madras; MG, Mangalore; MY, Mysore; SH, Shimoga; SN, Sandur; W, Wajrakarur; BKB, Bhima–Kaladgi Basin; CB, Cuddapah Basin; ChB, Chitradurga Basin; Ch, Charnockites; CG, Closepet Granite; DT, Deccan Traps; In, Intrusives; Km and Bb, Kudremukh and Bababudan Iron belts. Black patches represent iron-ore formations mapped from Project Vasundra. Schist belts: a, Raichur–Deodurg; b, Hutti–Muski; c, Hungund–Kushtagi; d, Veligullu–Ramagiri, and e, Kolar.

margin of the Cuddapah basin separating the Dharwar craton from the Eastern Ghats belt. South of the orthopyroxene isograd (south of 13°N), charnockitic rocks of the Southern Granulitic terrain are exposed.

Krishna river, with some of its most important tributaries, viz. the Bhima, Tungabhadra, Dharma, Kumudavati and Hemavati along with the Pennar and its tributaries, drains the area. The known faults and shears of the Peninsular shield closely follow the pattern of major rivers. Two dominant structural trends, viz. NE–SW to ENE–WSW and NNW–SSE to NW–SE traverse the region under study. The most important linear feature of the region is NNW–SSE-trending Chitradurga Boundary Shear (CBS). ENE–WSW-trending Krishna fault, Dharma–Tungabhadra fault, Kumudavati–Narihalla fault, Panjim fault, etc. are transverse to the tectonic grain of the terrain. These faults/lineaments and shear zones are discussed in the *Seismotectonic Atlas*⁷ and Project Vasundara³.

Aeromagnetic surveys over Peninsular India have been conducted by several agencies at different epochs and the prepared degree-sheet aeromagnetic contour maps are available with the GSI. The *Catalogue of Aerogeophysical Maps* published by GSI⁸ include details about the survey. Surveys were conducted over the Dharwar craton (74–78°E) in two blocks – the northern block (14–17°N) covered during the period 1987–89 at an altitude of 5000 ft and the southern strip (12–14°N) covered during 1984–85 at flight altitude of 7000 ft. The line spacing for all the blocks was maintained at 4 km. Aeromagnetic data were collected over the western part of Cuddapah basin and the adjoining crystallines at a flight altitude of 500 ft during 1980–81, with line spacing of 500–1000 m. Aeromagnetic data over the eastern segment of Cuddapah basin have been covered under Operation Hard Rock, but these data have not been purchased due to prohibitive cost and results in a data gap. The Eastern Ghats block (12–17°N, 78.5–81°E) was covered during 1983–87, with the altitude of survey being 5000 ft. The data are acquired with flight line direction of N25°E–S25°W for 7000 ft data and NS for the rest of the survey, and the flight lines were tied up individually to their respective tie-line set-up. The basic data presented in this paper are from the purchased degree-sheet aeromagnetic maps from GSI.

The analogue degree-sheet aeromagnetic total field anomaly maps, acquired from GSI, were digitized along contours at close interval for each degree-sheet to obtain the ASCII–XYZ files. The quality of digitization for each of the degree-sheets was checked by gridding and contouring the ASCII files individually and comparing it with the original degree-sheets. The degree-sheet maps were not corrected for the normal field. To correct for the contribution from the main core field, International Geomagnetic Reference Field (IGRF) up to degree and order 10 was used. The digitized aeromagnetic data are

corrected using the IGRF of the appropriate epoch, with the model being interpolated to the exact period and altitude of observation. Each of the IGRF-removed blocks were gridded at an interval of 2.5 km and continued to common datum of 7000 ft above msl. Minimum curvature random gridding was chosen for the digitized data sets, in view of the uneven distribution of data points. Since our interest is to throw light on the finer details, we have selected a close grid interval of 2.5 km. As the flight line spacing is 4 km, a grid interval of less than 2 km (related to Nyquist frequency) is likely to result in aliasing and give some spurious results. The data in the different blocks, continued to the same elevation, were then merged⁹ and a colour-shaded image map was produced (Figure 2).

The anomaly map (Figure 2) shows a combination of short to long wavelength anomalies. Many of the geological structures in the area are dramatically brought out in the image map. The Dharwar craton is mainly characterized by NW–SE anomaly patterns in the northern part, changing to almost N–S in the southern part, which is in accordance with the general Dharwarian trend. In addition, the Dharwar block depicts a few NE–SW trends. The NW–SE trends can be easily correlated to the greenstone and allied supracrustals seen in this craton. The NW–SE-trends show parallelism with the NW–SE-trending Godavari rift in the northeast. The most prominent features in this block are the NW–SE trending linear band of anomalies running from the northwestern corner of the map towards the Cuddapah basin. The linear features north of Sandur are respectively, the Sandur lineament (Sn) and the Wajrakarur lineament (Wk). The Wajrakarur lineament has a tectonomagmatic importance as major kimberlite pipes are known to exist in this region. The linear features north of Wajrakarur are respectively called as Raichur lineament (Rc), Bhima lineament² (Bh) and the Dindy fault (Df). While the Chitradurga basin is shown as detached patches, there is no clear evidence of the Closepet granite intrusive in the image map. Shimoga basin is characterized by gentle gradient, possibly reflecting the basement. Some of the 3D anomalies, high-amplitude closures, south of Sandur (IIID) and Shimoga (IVC) and near Panaji (IIB) can be easily correlated with the iron-ore belts of Bellary, Kudremukh, Bababudan and Goa respectively. Some distinct NE–SW features are also evident on the Dharwar craton, many of which are not brought out in the coarse grid map², suggesting that the sources of these anomalies are shallow or of limited lateral extent. The NE–SW features include the Panjim fault (Pf) and the continuation of Krishna river fault north of Wajrakarur. A distinct ENE–WSW-trending magnetic linear (IIC, IIIB), not having any surface geological manifestation appears to be cutting right across the craton, as shown in Figure 2. This linear may have major tectonic implications. The emplacement of kimberlite is believed to be controlled by

intersection of these NW–SE and NE–SW lineaments¹⁰. The anomalous zone in the northwestern corner of the map (IC) can possibly be associated with the trap cover of the Bhima and Kaladgi basins.

The trend of the anomalies within the block 12–13°N swerves from NW–SE in the west to NE–SW in the east through E–W in the central part. This can be easily correlated with the strike of the charnockitic rocks outcropping in this region. The NE–SW trending anomaly (VD), stretching from Mysore to Bangalore, can be associated with the Hunsur lineament³ representing deep-seated crustal fracture with which are associated emplacement of tholeiitic and acidic–alkaline dyke systems and granitoids. The Eastern Ghats block shows different trends. The Cuddapah basin is characterized by E–W-trending, high-amplitude broad anomaly and possibly reflecting the basement. The NW–SE-trending high-low-high pair (IIIF) in the southwestern margin of the Cuddapah basin represents basic–ultrabasic magmatism as well as mafic dyke swarms in the adjoining terrain. The northern and southern part of the Eastern Ghats block show typical NE–SW Eastern Ghats trend and can be easily explained as due to the strike trends of exposed and near-surface high-grade granulitic rocks.

The area under investigation is in the low-latitude region and the inclination of the inducing main field increases the complexity of the anomalies and makes the interpretation difficult. The analytical signal of the total field reduces the magnetic data to anomalies whose maxima mark the edges of the magnetized bodies¹¹. Hence analytical signal of the total field is calculated to delineate the source bodies. The absolute value of the analytical signal is defined as the square root of the squared sum of the vertical and the two horizontal derivatives of the magnetic field¹². Figure 3 is a plot of the analytical signal of the magnetic field, brown represents highs and blue depicts lows.

The iron-ore belts and the mafic flows associated with the eastern margin of Chitradurga schist belt are clearly brought out in the analytical signal map. The Chitradurga schist belt is bisected into two distinct parts with the southern part having two arms, with one arm shifted to the west. West of Chitradurga the prominent magnetic sources are the iron-ore formations of Bababudan, Kudremukh (IVC) and Goa (IIB). The NNW–SSE-trending magnetic sources below Panaji (IIIB) can possibly be related to the sub-surface iron-ore formation. Thus in the Western Dharwar block, iron-ore formations are forming a band running parallel to the coastline from north of Panaji and meet the magnetic source trends of the iron-ore formations of Bababudan and Kudremukh. The major magnetic sources to the east of Chitradurga are having NW–SE trend in the northern part changing to N–S in the south, with a convexity towards the east. The NW–SE-trending Kolar-type schist belts are associated with prominent magnetic sources. The Hungund–

Kustighi (IC, IID), Hutti–Muski (ID), Raichur–Deodurg (ID, IIE) belts to the north and Kolar and Veligullu–Ramagiri belts (IVF) to the south show magnetic response. From the analytical signal it seems that the Hungund–Kustugi and the Raichur–Deodurg belts extend further NW. Of these, the former extends underneath the Bhima and Kaladgi basins. The ENE–WSW (IIC, IIIB)-trending lineament and the composite batholithic complex of the Closepet granites are evident on the analytical signal map. Towards the Eastern Ghats mobile belt, the magnetic sources seen can be associated with the high-grade rocks, mainly charnockites, exposed and in the sub-surface towards the coast and the Nellore greenstone belt. It may be interesting to note that the region above Chennai (Madras) and below Kavali is characterized by low-intensity magnetic sources. South of 13°N, the analytical signal is associated with the charnockites mapped at the surface. The NE–SW-trending belt of the basic igneous rocks north of Mysore, finds expression in the analytical signal map.

The aeromagnetic total field anomaly map and its analytical signal map give a general idea about the distribution of magnetic sources in the Dharwar craton consistent with the known tectonic trend. Based on the nature of the anomaly trend, the area under investigation can be divided into three major blocks: the NNW–SSE-trending Dharwar block, E–W-trending high-grade terrain of the SGT block and the NE–SW-trending Eastern Ghats block. The Dharwar can be further divided into Eastern and Western blocks depending on the distribution of magnetic sources. The criterion adopted for this division is the presence of iron-ore. The magnetic anomaly sources in the Western block are mainly iron-ore, while in the Eastern block it reflects the gold-bearing schist belts. Keeping this in view, the magnetic data suggest that the Chitradurga schist belt, divides the Dharwar craton into the Western and Eastern blocks. A surprising result is that the schist belts in the Eastern block, not showing clear evidence in the published long wavelength map², are better defined in the present map, created using finer grid interval, implying their depth extent may be shallow.

The magnetic signature associated with the Western Dharwar block comprising the Shimoga, Chitradurga and the Sandur basins comes from the associated iron-ore formations, either exposed or in the sub-surface. Removing the signatures associated with iron-ore belts from the Western Dharwar results in a magnetically flat region with low gradient and low amplitude, possibly reflecting the basement. Analysing the nature of the anomalies suggests the basement to be composed of low-grade gneiss, consistent with several previous studies.

The magnetic response of the Eastern Dharwar block is surprisingly high, i.e. the density of high-amplitude anomalies is more. When compared with the Western block, the Eastern block has a paucity of ultramafic/

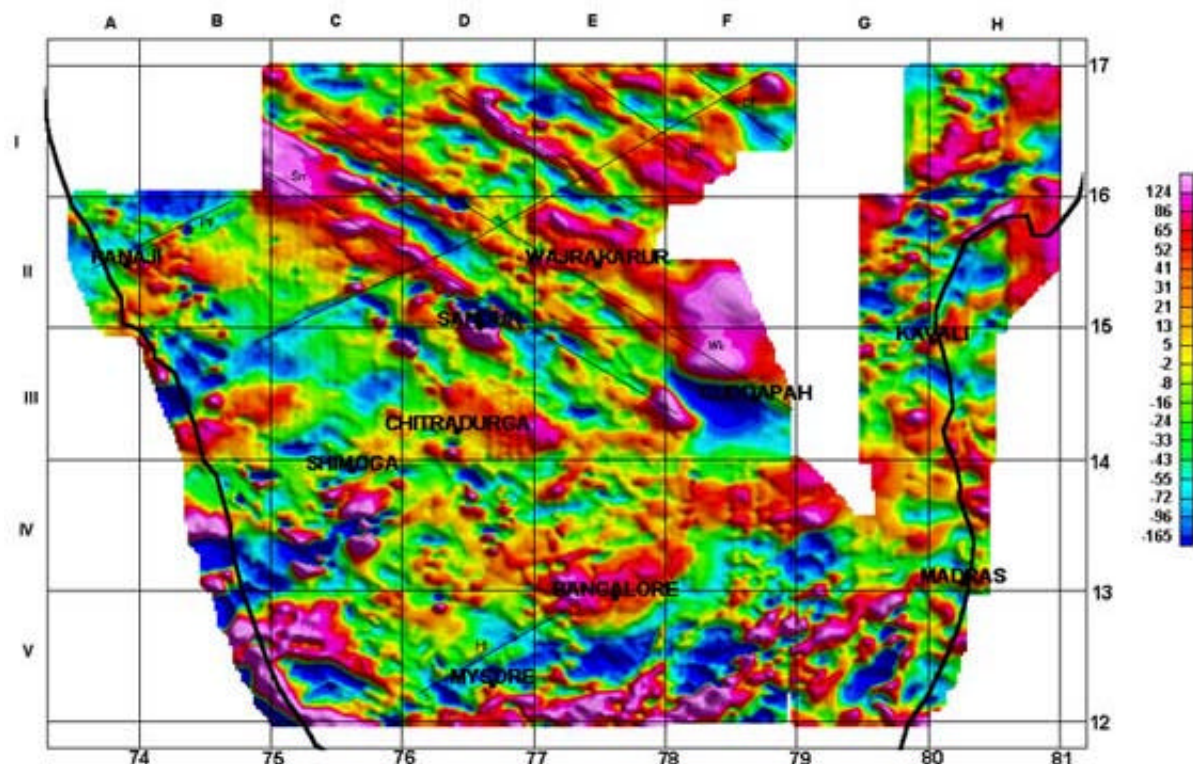


Figure 2. Total field magnetic anomaly image map of Dharwar craton. Inferred faults/lineaments are superposed. Pf, Panjim fault; Sn, Sandur lineament; Wk, Wajrakarur lineament; Rc, Raichur lineament; Bh, Bhima lineament; Df, Dindiy fault; and Hl, Hunsur lineament.

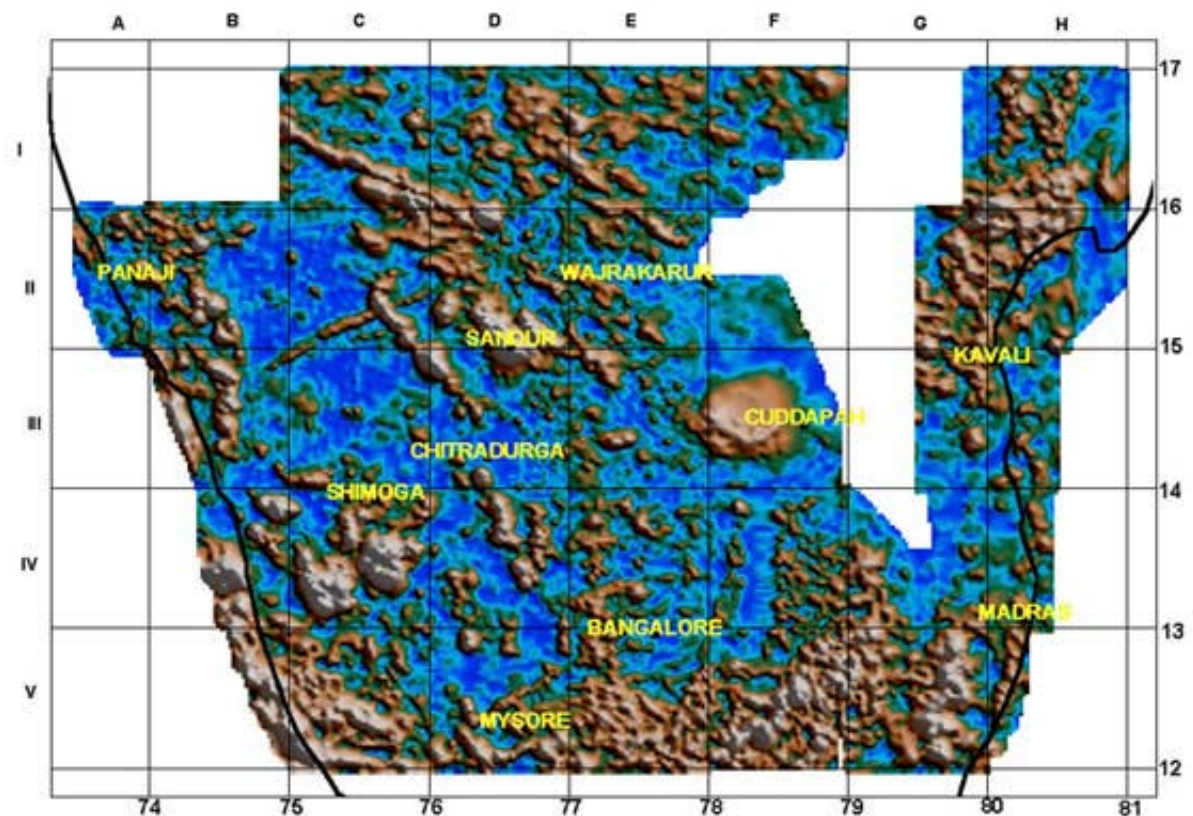


Figure 3. Analytical signal map of the total magnetic field anomaly. Brown colour represents highs and blue represents lows.

anorthositic layered complexes⁶ and lesser incidence of Banded Iron Formation. The difference in magnetic signature of the Eastern and Western blocks can be explained either in terms of the difference in environment of deposition and/or the difference in grades of metamorphism. This difference can be due to either or a combination of the following: (a) The Western Dharwar has a larger sedimentary component, while the Eastern is dominantly volcanic in origin. (b) Metamorphism affects the nature of iron compounds in rocks and thus affects susceptibility. The magnetic field of the Eastern Dharwar is consistent with a higher grade of metamorphism compared to the Western Dharwar. (c) The Eastern Dharwar craton might have been uplifted with respect to the Western Dharwar craton, with the characteristics of the deeper crustal layers now exposed by erosion.

Any theory of the evolution of the Dharwar craton should incorporate the difference between the Eastern and the Western Dharwar, as evidenced from different data sets: magnetic, geology, gravity, heat flow, radiometric dating, seismic, magneto-telluric, etc.

1. Pichamuthu, C. S., *J. Geol. Soc. India*, 1962, **3**, 106–118.
2. Harikumar, P., Rajaram, M. and Balakrishnan, T. S., *Proc. Indian Acad. Sci. (Earth Planet. Sci.)*, 2000, **109**, 381–391.
3. Project Vasundhara, Special Publication AMSE Wing, Geological Survey of India, Bangalore, 1994.
4. Swami Nath, J., Ramakrishnan, M. and Viswanatha, M. N., *Rec. Geol. Surv. India*, 1976, **107**, 149–175.
5. Subrahmanyam, C. and Verma, R. K., *Tectonophysics*, 1982, **84**, 225–245.
6. Radhakrishna, B. P. and Vaidyanadhan, R., Text Book Series, No. 6, Geol. Soc. India, 1997, p. 354.
7. Geological Survey of India, *Seismotectonic Atlas of India and its Environs*, 2000.
8. Geological Survey of India, *Catalogue of Aerogeophysical Maps*, Airborne Mineral Surveys and Exploration Wing, Bangalore, India, 1995.
9. Johnson, A., Cheeseman, S. and Ferris, J., *Ann. Geofis.*, 1999, **42**, 249–259.
10. Nayak, S. S., Kasiviswanatham, C. V., Reddy, T. A. K. and Nagaraja Rao, B. K., *J. Geol. Soc. India*, 1989, **31**, 343–346.
11. MacLeod, I. N., Jones, K. and Dai, T. T., *Explor. Geophys.*, 1993, **24**, 679–687.
12. Roset, W. E., Verhoef, J. and Pilkington, M., *Geophysics*, 1992, **57**, 116–125.

ACKNOWLEDGEMENTS. The aeromagnetic data used in this paper were purchased as part of a DST–Deep Continental Studies (DCS) project. Financial assistance received from DST is gratefully acknowledged.

Received 8 November 2001; revised accepted 1 May 2002

Thermospheric temperature and magnetic field measurements from Mt Abu during a geomagnetically disturbed period – a case study

D. Chakrabarty*[†], Tarun K. Pant[#], R. Sekar*, Alok Taori*, N. K. Modi* and R. Narayanan*

*Physical Research Laboratory, Ahmedabad 380 009, India

[#]Space Physics Laboratory, Vikram Sarabhai Space Centre, Thiruvananthapuram 695 022, India

During the recovery phase of a ‘moderate’ geomagnetic storm, spectroscopically measured night-time thermospheric temperatures from Mt Abu (24.6°N, 73.7°E, dip 19.09°) are found to deviate considerably (~200–600 K) from the MSIS-90 model temperatures on many occasions, implying the model’s limitations as applied to low-latitude thermosphere. The measured temperatures exhibit oscillatory features as opposed to the flat, featureless temperature profiles rendered by the MSIS-90 model. The temperature variabilities are found to succeed the variations in the time rate of change of the total magnetic field measured by a standard Proton Precession Magnetometer by ~12.5 h, revealing the ‘response time’ of the low-latitude thermosphere to the disturbances over higher latitudes.

HIGH-resolution spectroscopic measurements of the thermospheric temperatures from the broadening of the OI 630.0 nm atomic oxygen line (O¹D–O³P) are widely used to decipher the kinetic temperature of the neutral thermosphere. It is known that a Fabry–Perot (FP) spectrometer is an ideal device for such measurements owing to its large light-gathering power at high spectral resolution¹. Most of the earlier measurements were concentrated on mid and high latitudes and measurements from low-equatorial latitudes are rather sparse^{2–4}. However, with the advent of multi-instrumented, coordinated investigations using space as well as ground-based platforms, it is now understood that the neutral thermosphere and the ionized ionosphere do not act in isolation, and they are coupled by various electro-dynamical and neutral dynamical processes. Thermospheric temperature data from a low-latitude station can be very useful to understand the various coupling (energetic as well as dynamic) aspects of the high and low latitude thermosphere–ionosphere system (TIS) during varying geophysical conditions.

During geomagnetic storms, large amount of energy gets injected in the high-latitude region primarily in the form of energetic particle precipitation. This excess energy then gets redistributed through meridional wind circulation (owing to the pressure difference between the

[†]For correspondence. (e-mail: dipu@prl.ernet.in)